Multistep autoactivation of asparaginyl endopeptidase in vitro and in vivo

Li, Dongtao Ni; Matthews, Stephen P.; Antoniou, Antony N.; Mazzeo, Daniela; Watts, Colin

Published in:
Journal of Biological Chemistry

DOI:
10.1074/jbc.M305930200

Publication date:
2003

THE JOURNAL OF BIOLOGICAL CHEMISTRY
Vol. 278, No. 40, Issue of October 3, pp. 38980–38990, 2003
Printed in U.S.A.

Multistep Autoactivation of Asparaginyl Endopeptidase *in Vitro* and *in Vivo**

Received for publication, June 5, 2003, and in revised form, July 9, 2003
Published, JBC Papers in Press, July 14, 2003, DOI 10.1074/jbc.M305930200

Dongtao Ni Li‡, Stephen P. Matthews‡, Antony N. Antoniou, Daniela Mazzeo, and Colin Watts§

From the Division of Cell Biology & Immunology, Wellcome Trust Biocentre, School of Life Sciences, University of Dundee, Dundee, DD1 5EH, United Kingdom

Mammalian asparaginyl endopeptidase (AEP) or legumain is a recently discovered lysosomal cysteine protease that specifically cleaves after asparagine residues. How this unusually specific lysosomal protease is itself activated is not fully understood. Using purified recombinant pro-enzyme, we show that activation is autocatalytic, requires sequential removal of C- and N-terminal pro-peptides at different pH thresholds, and is bimolecular. Removal of the N-terminal propeptide requires cleavage after aspartic acid rather than asparagine. Cellular processing, either of exogenously added AEP precursor or of pulse-labeled endogenous precursor, introduces at least one further cleavage to yield the final mature lysosomal enzyme. We also provide evidence that in living cells, there is clear compartmental heterogeneity in terms of AEP activation status. Moreover, we show that human monocyte-derived dendritic cells harbor inactive proforms of AEP that become activated upon maturation of dendritic cells with lipopolysaccharide.

Asparagine endopeptidase (AEP),[1] also known as legumain, is a lysosomal cysteine protease that cleaves protein substrates on the C-terminal side of asparagine (1). This strict specificity is unusual among lysosomal enzymes (2). The recent discovery of this enzyme in mammals followed earlier identification of similar enzymes (initially termed "vacuolar processing enzyme" or VPE) in plants (3–5) and in *Schistosoma mansoni* (6, 7). AEP/legumain is unrelated to the papain-like C1 family of lysosomal cysteine proteases such as cathepsins S, B, L, and H but has features that suggest an evolutionary relationship to the caspases, the bacterial proteases gingipain and clostripain, and separase (8, 9).

AEP is expressed in diverse cell types, and in most cases its functions are still unknown. AEP has emerged as an important enzyme in antigen and autoantigen processing, targeting selected asparagine residues in tetanus toxin, myelin basic protein, and other antigens (10–14). In the case of the tetanus toxin C fragment, AEP introduces a small number of cleavages that "unlock" the folded protein substrate, making it available for class II MHC binding and, potentially, additional protease action (11, 15).[2] In contrast, we have shown that AEP action on myelin basic protein can destroy a T cell epitope, preventing its display on class II MHC molecules and possibly the elimination of autoreactive T cells specific for this epitope (12). AEP can initiate processing of the invariant chain, although this key event in class II MHC maturation can also be performed by other enzymes (16). AEP/legumain has also been implicated in the activation of pro-gelatinase A (17), in α-thymosin processing (18), and as an inhibitor of osteoclast formation (19). Very recently, analysis of mice deficient in AEP demonstrated an accumulation of the single chain forms of cathepsins H, B, and L, changes in the activities of several lysosomal exopeptidases, and age-dependent perturbation of kidney proximal tubule lysosome function (20).

Thus AEP is emerging as a lysosomal enzyme whose specificity makes it ideal for the limited cleavages necessary for pro-protein processing and antigen presentation. How AEP is itself activated is of some interest because this may in turn control the activation/processing of downstream substrates including other lysosomal proteases. Like several members of the papain family of lysosomal cysteine proteases, activation of AEP is triggered by acidic pH and appears to be autocatalytic (21–23). In the case of the *Arabidopsis* enzyme (γVPE), Kuroyanagi *et al.* (21) have shown that sequential removal of C- and N-terminal propeptides by cleavage after Asn occurs, although removal of the N-terminal peptide was not necessary for activity. Other plant VPEs may autoactivate through cleavages after aspartic acid (22). However, somewhat incomplete and conflicting data have appeared regarding the mechanism of autoactivation of mammalian AEP. One report documented autoactivation of an AEP-Ig fusion protein following cleavage after one or more aspartic acid residues (24). Another study, which followed the activation of pro-AEP in cell lysates, reported an obligatory cleavage after asparagine 323 leading to enzyme activation (25).

Here we analyze the autoactivation pathway of pro-AEP *in vitro* and *in vivo*. We show that sequential cleavages after both asparagine and aspartic acid are necessary for efficient enzyme activation resulting in the removal of a 110-residue C-terminal and a short 8-residue N-terminal pro-peptide, respectively. The key activating cleavage at Asp^{25} only occurs below pH 5.0 and yields active enzyme, which is, however, still significantly larger than the final cellular form of AEP. The fully mature form is generated by living cells either from endogenous pro-AEP or following endocytosis and cellular processing of recombinant pro-AEP. AEP biosynthesis is induced as blood mono-

* This work was supported by Medivir UK Ltd. and the Wellcome Trust. The costs of publication of this article were defrayed in part by the payment of page charges. This article must therefore be hereby marked "*advertisement*" in accordance with 18 U.S.C. Section 1734 solely to indicate this fact.

‡ These authors contributed equally to this work.
§ To whom correspondence should be addressed. Tel.: 44-1382-344233; Fax: 44-1382-345783; E-mail: c.watts@dundee.ac.uk.

[1] The abbreviations used are: AEP, asparagine endopeptidase; VPE, vacuolar processing enzyme; MHC, major histocompatibility complex; CHO, Chinese hamster ovary; Z, benzyloxycarbonyl; NHMec, 7-(4-methyl)coumarylamide; Fmoc, *N*-(9-fluorenyl)methoxycarbonyl; CHAPS, 3-[(3-cholamidopropyl)dimethylammonio]-1-propanesulfonic acid; DC, dendritic cell(s); LPS, lipopolysaccharide; DHFR, dihydrofolate reductase.

[2] C. Moss and C. Watts, unpublished observation.

cytes are differentiated into dendritic cells, but only partial activation occurs. Maturation with LPS triggers the appearance of fully mature and active enzyme. This multi-step, pH-regulated activation pathway may therefore be used to control processing capacity for antigens and other AEP substrates.

MATERIALS AND METHODS

Cloning and Expression of the AEP Precursor—Total RNA was prepared from the EBV B cell line 4.2 (26) using RNAzol according to the manufacturer's conditions and used as template for reverse transcription-PCR. Specific AEP cDNA was generated using avian myeloblastosis virus reverse transcriptase and the reverse primer 5′-CCGCTCGAGAAGCTTTCAGTAGTGACCAAGGCACAC-3′ and subsequently amplified using forward primer 5′-CCGGAATTCATGGTTTGGAAAGTAGCTGTATTCCTC-3′ and reverse primer 5′-CCGCTCGAGAAGCTTTCAGTAGTGACCAAGGCACAC-3′ under the following PCR conditions: 1 cycle of 95 °C for 2 min; 15 cycles of 94 °C for 30 s, 65 °C for 30 s (decreasing by 1 °C/cycle), and 68 °C for 3 min; 25 cycles of 94 °C for 30 s, 50 °C for 30 s, and 68 °C for 3 min (+10 s/cycle); and 1 cycle of 68 °C for 10 min. AEP cDNA was gel-extracted and ligated using T4 DNA ligase into pCR3 vector (Invitrogen) using the *Xho*I and EcoR1 restriction sites underlined in the above primers. To generate a suitable vector for methotrexate-driven AEP overexpression the AEP insert was reamplified to include an optimal Kozak sequence at the 5′ end and a His_6 C-terminal tag using forward primer 1 (5′-ACGATATCACCATGGTTTGGAAAGTAGCTGTATTCC-3′) and reverse primer 1 (5′-ATCTAGAGAATTCGCGGCCGCTCAATGGTGATGGTGATGGTGGTAGTGACCAAGGCACACGTG-3′). The product was cloned into the *Eco*RV and *Not*I sites (underlined in primers) of vector pcDNA DHFR (27) to generate the AEP expression vector pDT1. $DHFR^-$ CHO cells (European Collection of Animal Cell Cultures, UK) were transfected using the calcium phosphate method, and colonies were initially selected in Iscove's medium lacking thymidine and hypoxanthine plus dialyzed fetal calf serum. After ~2 weeks the surviving colonies were subjected to further selection in 20 nM methotrexate followed by stepwise increases to 100 nM, 500 nM, and finally 1 μM. Single colonies were picked at 100 nM. The conditioned medium (5 μl) and cell lysates (15 μg) were screened by Western blotting using an anti-human AEP antibody raised in sheep (10). More than 20 overproducing cell lines were isolated in this way. For most experiments we used clones 2C3 or 3A5. We estimated up to 70-fold overexpression of active AEP within the cells and up to 10–20 mg/liter of AEP precursor secreted into the growth medium (see Fig. 1). For production of the AEP precursor, the overproducing cells were adapted to CHO-S-SFMII serum-free medium (Invitrogen) by progressive reduction in the level of fetal calf serum (10%, 5%, 2.5%, 1%, and then 0%) with each step taking about 1 week. To purify the AEP precursor, up to 1 liter of medium, conditioned by cell growth for approximately 1 week, was adjusted to 1 M NaCl and passed over a nickel-agarose column. The column was washed with Tris, pH 7.4, 1 M NaCl, 10 mM imidazole. The AEP precursor was eluted in the same buffer containing 0.5 M imidazole, dialyzed against phosphate-buffered saline and stored at −20 °C in 20% glycerol.

AEP Autoactivation and Assay Conditions—Autoactivation of AEP was performed by diluting aliquots of the 56-kDa AEP precursor into a buffer containing 0.2 M sodium citrate/citric acid plus 1 mM dithiothreitol adjusted to different pH values. After different time periods at 37 °C, AEP enzyme activity was assessed by transferring aliquots of the autoactivation reaction to AEP assay buffer (28), which included 10 μM Z-Ala-Ala-Asn-NHMec as substrate. Release of NHMec was measured using a Cytofluor plate reader. Note that the pH of the assay buffer (pH 5.8) is optimal for AEP activity measurement but prevents autoactivation, which requires lower pH values. AEP autocatalytic cleavage sites were identified following transfer of 56-, 47-, 46-, and 11-kDa products to polyvinylidene difluoride membrane followed by eight cycles of Edman degradation in an ABI sequencer.

The N-terminal propeptide VPIDDPED and its variant forms (synthesized by Dr. G. Bloomberg, Bristol University) were dissolved in water to a final concentration of 50 mg/ml, and the pH was adjusted by the addition of 2 M NaOH. Different concentrations were tested either on preactivated 46-kDa AEP or for their ability to inhibit the autoactivation of 56-kDa AEP. For the inhibition of autoactivation experiments, the 56-kDa AEP protein was incubated at pH 4.0 at a concentration of 0.5 $mg \cdot ml^{-1}$ in the presence of the reversible inhibitor Fmoc-AENK-amide or a control peptide, Fmoc-AEQK-amide. The autoactivation reaction was stopped by diluting into pH 5.8 buffer and further diluted into assay buffer for measurement of AEP enzyme activity. The final concentration of inhibitor peptide in the assay buffer was 2.3 μM, *i.e.* less than 10% that of the Z-Ala-Ala-NHMec substrate, which was adjusted to 25 μM.

Site-directed Mutagenesis—Mutagenesis of Asp^{21} and Asp^{25} to alanine in pro-AEP was performed by PCR using forward primer 1 (see above) and mutagenic reverse primers that incorporated a unique *Dra*III site (underlined) located immediately downstream of the Asp^{25} codon: Reverse 2, 5′-GATCACCACCCAGTGCTTGCCTCCATCTTCAGGATC**AGC**TATAGGAAC-3′ changing Asp^{21} to Ala; Reverse 3, 5′-GATCACCACCCAGTGCTTGCCTCC**AGC**TTCAGGATCATCTATAGGAAC-3′ changing Asp^{25} to Ala^{25}; and Reverse 4, 5′-GATCACCACCCAGTGCTTGCCTCC**AGC**TTCAGGATC**AGC**TATAGGAAC-3′ changing both Asp^{21} and Asp^{25} to Ala. The PCR products were introduced into pDT1 by fragment exchange utilizing *Eco*RV and *Dra*III restriction sites. Substitution of Cys^{189} and of Asn^{323} with Ser and Ala, respectively, was achieved using the QuikChange kit (Stratagene). All of the constructs were checked by DNA sequencing.

Expression of Mutant AEPs—The AEP mutants were expressed in 293T cells by transient transfection using Ca^{2+}-phosphate. After 17–20 h the medium was replaced with fresh medium (Dulbecco's modified Eagle's medium, 25 mM Hepes, 10% fetal calf serum). Two days later the serum level was reduced to 5%, and medium was collected after 3–5 days. AEP mutants were purified by nickel-agarose chromatography as described above. Autoactivation conditions were as above at pH 4.0 or pH 4.5 for 2–5 h.

Antibodies—Antisera production was performed under contract with Diagnostics Scotland (Carluke). Sheep and mice were immunized with a mixture of 56-kDa AEP precursor and fully autoactivated 46-kDa AEP. Rabbits were immunized with the N-terminal peptide VPIDDPEDGGKHWV coupled through a C-terminal cysteine residue to maleimide-activated keyhole limpet hemocyanin. After two successive boosts, both the rabbit and sheep antibodies were affinity purified on the same peptide coupled to Sulfolink gel (Pierce). The sheep antibodies were subjected to repeated rounds (four in all) of purification until the reactivity to activated forms of AEP was removed. This antibody is named αAEP_{18-31}. Sheep antibodies were also affinity purified on immobilized 56-kDa AEP. Murine monoclonal antibodies were obtained by standard methods, screened by enzyme-linked immunosorbent assay, Western blotting, and immunofluorescence microscopy and were recloned twice.

Radiolabeling of 56-kDa AEP and [^{35}S]Met/Cys Pulse-Chase Labeling—Purified 56-kDa AEP precursor (6–10 μg) was radioiodinated in a final volume of 20 μl of 0.25 M sodium phosphate, pH 7.2 containing 0.5 mCi of ^{125}I. After 15 min the reaction was terminated by the addition of 5 μl of 20 mM tyramine and 5 μl of 1 M KI. The labeled protein was isolated by chromatography on a 10-ml PD-10 column (Amersham Biosciences). To detect uptake of ^{125}I-AEP by wild type CHO cells, 10^6 cells were seeded in 6-well culture plates, and 0.2 μg/ml ^{125}I-AEP was added in a final volume of 2 ml complete Dulbecco's modified Eagle's medium. Where indicated, inhibitors were added 1 h before the addition of ^{125}I-AEP. After different times the cells were washed with ice-cold phosphate-buffered saline, detached with phosphate-buffered saline with 10 mM EDTA, and collected by centrifugation. After two more washes, the cells were lysed in AEP assay buffer (28) but containing 1% CHAPS, 0.5% Triton instead of 0.1% CHAPS. The nuclei were removed by centrifugation, and the supernatant was analyzed by SDS-PAGE and autoradiography. In some experiments, labeled AEP was immunoprecipitated from postnuclear supernatants with affinity-purified antisera raised either in sheep or in rabbits. For [^{35}S]Met/Cys labeling, the 3A5 overproducing cell line was preincubated in RPMI 1640 lacking methionine and cysteine plus 10% dialyzed fetal calf serum for 1 h. 5×10^6 cells were labeled with 0.25 mCi of [^{35}S]Met/Cys (Amersham Biosciences) for 5 min. The medium was removed, and after washing the cells were chased in complete Dulbecco's modified Eagle's medium including 5 mM methionine. After different times the cells were washed and lysed at 0 °C in 20 mM Tris, pH 7.0, 0.15 M NaCl, 1% Triton X-100, 5 mM $MgCl_2$ plus protease inhibitors (Complete mixture; Roche Applied Science). After centrifugation to remove nuclei, labeled AEP was immunoprecipitated as above and analyzed on 12% Bis-Tris gels (NuPAGE; Invitrogen).

Dendritic Cell (DC) Culture—Blood from healthy donors was used to prepare peripheral blood monocytic cells. $CD14^+$ monocytes were isolated with magnetic beads (Miltenyi) according to the manufacturer's protocol and cultured at 4×10^5/ml with 800 units/ml granulocyte macrophage colony-stimulating factor (Leucomax, Sandoz) plus 1000 units/ml interleukin-4 (BD Biosciences) essentially according to the protocol of Sallusto and Lanzavecchia (29). DCs were CD1a-positive, and expression of CD86 and class II MHC increased following LPS-driven maturation (1 μg/ml; Sigma).

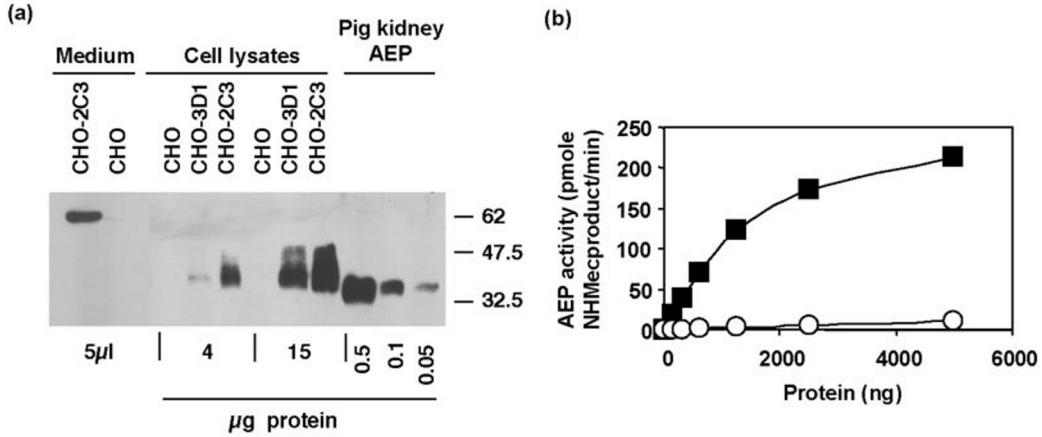

FIG. 1. **Overexpression of AEP in CHO cells.** *a*, Western blot of culture medium and cell lysates from untransfected CHO and AEP-overexpressing CHO lines. Known amounts of pig kidney AEP were run in parallel for comparison. Note that the antiserum used (10) is raised against the human AEP peptide KGIGSGKVLKSGPQ but cross-reacts with the pig sequence KGKGSGKVLKSGPR. *b*, comparison of hydrolysis of Z-AAN-NHMec by lysates of untransfected CHO (*open circles*) and CHO-3A5 (*filled squares*) cells that overexpress AEP.

Microscopy—MelJuSo-SD1 cells were seeded onto poly-L-lysine-coated coverslips and cultured overnight before fixing in 3% paraformaldehyde. The cells were permeabilized with 0.05% Triton X-100 and after preblocking with 0.2% fish skin gelatin, stained with sheep anti-AEP, sheep anti-AEP_{18-31}, mouse anti-AEP monoclonal antibodies 6E3 and 11B7, anti-LAMP-1 (Pharmingen), or combinations thereof. Secondary antibodies were donkey anti-sheep AlexaFluor 488 or donkey anti-mouse AlexaFluor 594 (Molecular Probes). Microscopy was performed on a Zeiss LSM 510 microscope.

RESULTS

Production and Purification of Homogenous AEP Proenzyme—To resolve some of the issues concerning the autoactivation of asparaginyl endopeptidase, we developed an expression system that permitted the purification of large amounts of the proenzyme. We took advantage of the potential that gene amplification offers in CHO cells for protein overproduction (30). The AEP cDNA was cloned into the vector pcDNA DHFR (27), $DHFR^-$ CHO cells were transfected, and initial selection was performed as described under "Materials and Methods." Selected colonies were then subjected to stepwise selection with increasing concentrations of the DHFR inhibitor methotrexate until the desired level of AEP production had been achieved. Amplification of the DHFR gene was confirmed by fluorescence-activated cell sorter analysis of cells labeled with fluorescinated methotrexate (Ref. 31 and data not shown), and parallel AEP overproduction was demonstrated by Western blotting of both the cells and growth medium. As shown in Fig. 1 AEP was readily detected in 5 μl of conditioned growth medium and in cell lysates from various selected clones. Parallel electrophoresis of purified pig kidney AEP indicated that overproduction in the cells was considerable (Fig. 1*a*). The AEP protein found in the growth medium was the proenzyme (56 kDa). We found no evidence of secretion of the mature enzyme (36 kDa), which was confined to cell lysates and migrated somewhat more slowly than purified mature pig kidney enzyme run in parallel (Fig. 1). To estimate the overproduction of AEP more accurately, we measured the hydrolysis of the AEP substrate Z-Ala-Ala-Asn-NHMec by CHO cell lysates. As shown in Fig. 1*b*, the initial rates of hydrolysis of this substrate indicated that at least 40-fold overproduction of active enzyme had been achieved in the cell lysates alone. We included a C-terminal histidine tag to aid purification of the proenzyme from CHO cell supernatants.

Stepwise Autoactivation of AEP at Acidic pH—We next attempted to autoactivate the purified proenzyme. As shown in the Coomassie Blue-stained gels in Fig. 2*a*, exposure to pH values in the range 6.0–5.5 resulted in the partial disappearance of the 56-kDa precursor and the appearance of 47- and 11-kDa products. Interestingly, little enzyme activity appeared, even at pH 5.0 where a significant amount of the 56-kDa precursor became converted. Similarly, below pH 3.5 we observed conversion of the 56-kDa precursor, but again enzyme activity failed to appear. As shown in Fig. 2*b*, active enzyme only appeared in a pH "window" between 4.5–3.5 and paralleled a small but clear increase in mobility of the major product of autocatalysis from 47 to 46 kDa (Fig. 2*a*). We sequenced the N termini of all the products generated at pH 5.8 and 4.5. As shown in Fig. 2*a*, whereas the inactive 56- and 47-kDa forms of AEP had the N-terminal sequence VPIDDP, the active 46-kDa form of AEP began with the sequence GGKHWV. Thus the inactive 47-kDa form of AEP was extended by 8 residues at the N terminus compared with the active 46-kDa form (Fig. 2*c*). We also sequenced the smaller 11-kDa processing product generated over a wide range of pH values (Fig. 2*a*). This product began with the sequence DLEESR demonstrating autocatalytic cleavage after Asn^{323} as previously reported by Chen and colleagues (25). However, in our hands it appeared to be the subsequent N-terminal cleavage after Asp^{25} that led to enzyme activation (Fig. 2 and see below).

The Final Step in AEP Maturation Is Not Autocatalytic but Occurs Following Normal Cellular Processing—AEP found in living cells has a mass of ~36 kDa, considerably smaller than the autocatalytically activated 46-kDa material. No processing beyond the 46-kDa product occurred *in vitro* even upon prolonged incubation. To test whether the purified recombinant 56-kDa proenzyme was capable of being fully processed by living cells, we labeled it with ^{125}I and offered this as a substrate for endocytic capture and processing by living CHO cells. We anticipated that the secreted 56-kDa precursor would still carry the necessary targeting signals, most likely mannose-6-phosphate, and that they might be recognized by receptors cycling between the cell surface and endosomes (32). As shown in Fig. 3*a* (*left panel*) the radioiodinated 56-kDa precursor autoactivated normally to the 46-kDa form *in vitro*. After 1, 3, and 6 h of incubation with ^{125}I-56kDa AEP, CHO cells were harvested, and accumulation of radiolabeled AEP was assessed by SDS-PAGE. As shown in Fig. 3*a* (*right panel*), the labeled proenzyme was taken up and converted to the 36-kDa mature form. There was little accumulation of either the 56-kDa or intermediate 47/46-kDa forms of AEP, indicating rapid cellular processing. Thus the recombinant pro-enzyme is capable of being rapidly and fully processed to the final 36-kDa form when

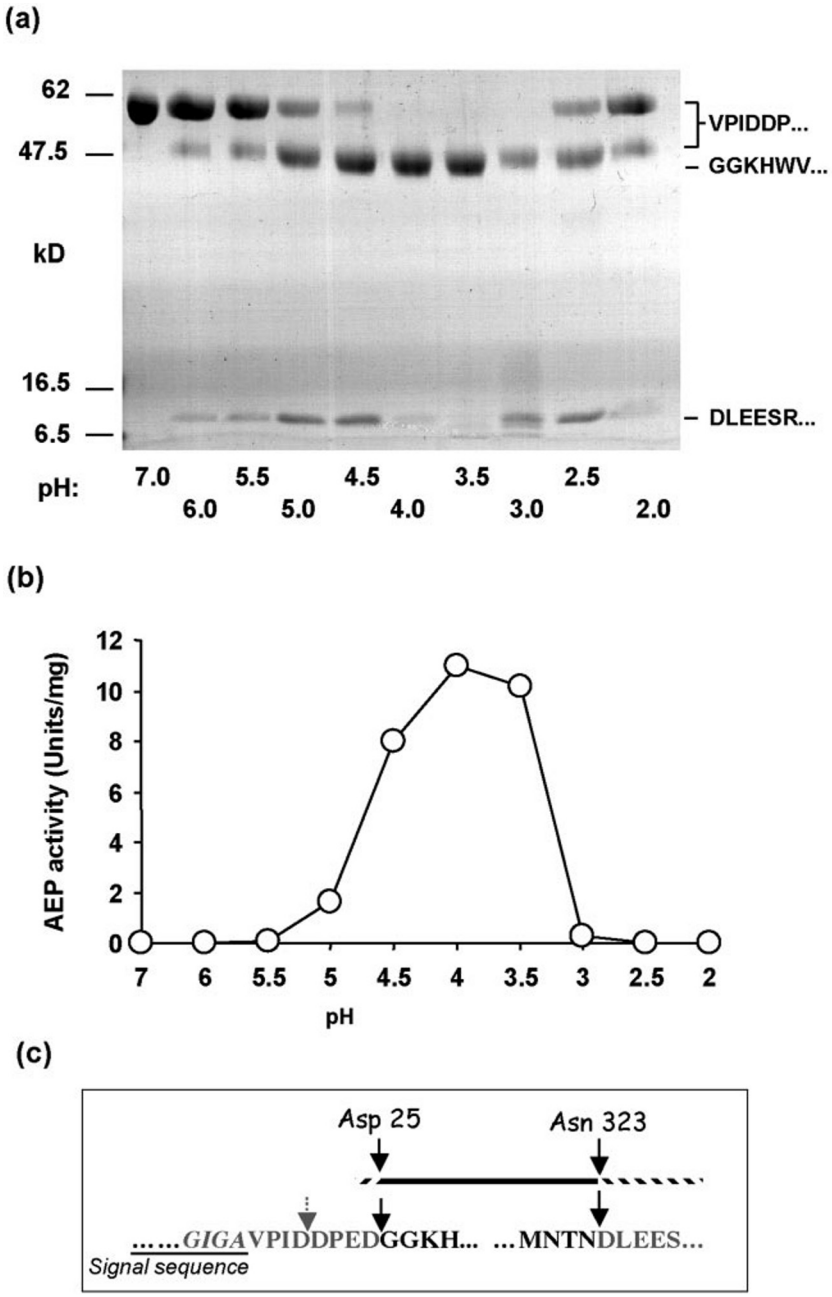

FIG. 2. **Autoactivation of the AEP protease.** *a*, purified AEP precursor was incubated at the pH values indicated for 2 h at 37 °C. Aliquots of each reaction were analyzed by SDS-PAGE (12%) and stained with Coomassie Blue. N-terminal Edman sequencing of each product gave the sequences shown on the *right*. *b*, a second aliquot was analyzed for ability to hydrolyze the Z-AAN-NHMec substrate. *c*, schematic of autocatalytic cleavages observed. Cleavage after Asn^{323} removes a 110-residue C-terminal propeptide (see also Ref. 25). A second cleavage after Asp^{25} removes an 8-residue N-terminal propeptide. In some experiments the sequence DPEDG was detected indicating cleavage at Asp^{21}.

added exogenously to living cells. We conclude that final maturation of AEP is most likely not autocatalytic but mediated by other lysosomal proteases. However, the identity of these enzymes remains uncertain. Neither leupeptin, E64 (Fig. 3*a*), or pepstatin (not shown) had much impact on the maturation of 56-kDa AEP, although in some experiments evidence of accumulation of a form slightly larger than 36 kDa was obtained with high concentrations of leupeptin (Fig. 3*a*). These inhibitors were active because the 11-kDa C-terminal propeptide accumulated to a greater extent in leupeptin and E64-treated cells (Fig. 3*a*). In addition, there was a noticeable increase in the amount of 56-kDa precursor associated with the cells. We suggest that a small proportion of the iodinated 56-kDa precursor fails to autoactivate and that this material is normally destroyed by leupeptin- and E64-sensitive lysosomal proteases that also degrade the 11-kDa C-terminal propeptide.

We were surprised to find no evidence for intermediate 46/47-kDa forms of AEP in the experiments described above. Most likely in the minimum time needed (1 h) to see accumulation of endocytosed AEP, conversion has already occurred. To establish that the 47- and 46-kDa forms are *bona fide* intermediates in AEP autoactivation in living cells, we also examined the maturation of biosynthetically labeled AEP. To distinguish between inactive (56 and 47 kDa) and active (46 and 36 kDa) forms of AEP, we raised an antiserum in rabbits against a synthetic peptide corresponding to the N terminus of the 56/47-kDa forms and a sheep antiserum that recognizes all forms of AEP. As expected, the rabbit serum did not recognize the active 46-kDa (or 36-kDa) species, whereas the sheep serum did (Fig. 3*b*). The AEP-overexpressing CHO cell line 3A5 was pulsed with [^{35}S]Met/Cys for 5 min and chased for various times, and the status of AEP was examined by sequential immunoprecipitation with the rabbit followed by the sheep antiserum. After the short pulse, most of the AEP migrated at the 56-kDa precursor size and over a 4-h period chased to the fully mature 36-kDa form, which was precipitated by the sheep but not the rabbit serum (Fig. 3*c*). However, the rabbit serum, raised against the N-terminal peptide, was able to precipitate a

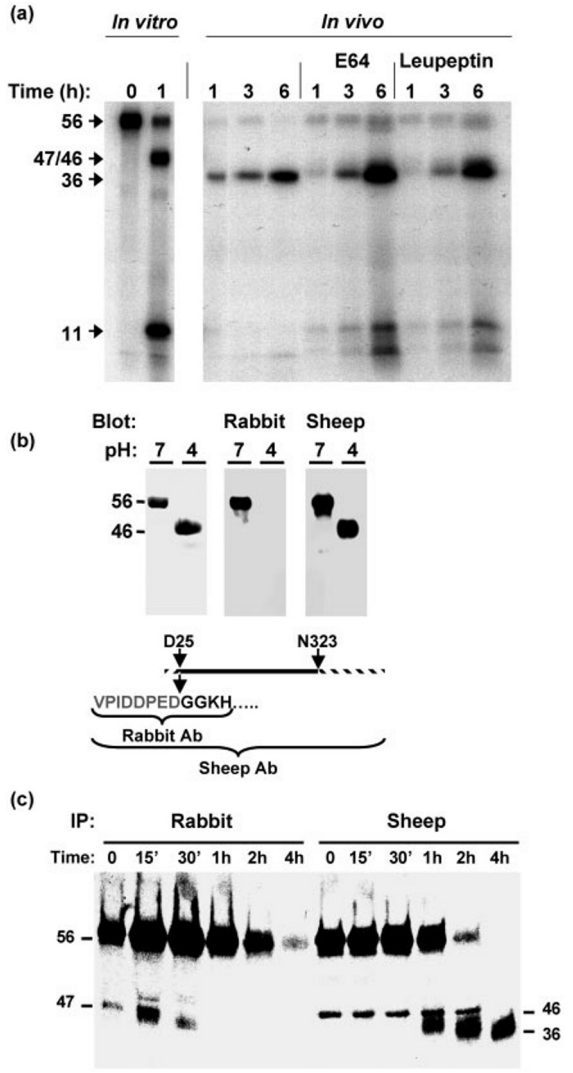

FIG. 3. **AEP maturation in living cells.** *a*, ^{125}I-labeled 56kDa AEP precursor (0.2 μg/ml) was added to living CHO cells for the times indicated with or without the cysteine protease inhibitors E64 (0.1 mM) or leupeptin (1 mM). Capture and maturation of AEP was assessed by SDS-PAGE and autoradiography. The ability of the radioiodinated 56-kDa precursor to autoactivate *in vitro* is shown in the leftmost two tracks. *b*, to verify the specificity of the two affinity-purified antisera, 56- and 46-kDa AEP were transferred to nitrocellulose, probed with the rabbit (N terminus-specific) antiserum, and revealed using a peroxidase-conjugated secondary. The blot was stripped and reprobed with the sheep antiserum. The corresponding Coomassie-stained gel is shown on the *left*. *c*, pulse (5 min) and chase (times shown) analysis of AEP maturation in CHO-3A5 cells. AEP products were immunoprecipitated (*IP*) as shown and analyzed by SDS-PAGE.

processed form of AEP that appeared transiently after 15 min of chase and that migrated around 47 kDa (Fig. 3*c*). Thus the C-terminally processed but N-terminally intact 47-kDa intermediate seen *in vitro* is also seen in living cells. Intermediates between the 46/47-kDa forms and the 36-kDa form were seen in this and other experiments, suggesting that the 36-kDa form may arise by processive C-terminal trimming of the 46-kDa form (Fig. 3*c*). As noted above, however, the enzyme or enzymes involved remain to be identified. In addition, this additional processing seems not to alter enzyme activity because the specific activity of 46-kDa human AEP activated *in vitro* was very similar to that of the fully mature 36-kDa enzyme purified from pig kidney (1 and data not shown).

Cleavage at Asp^{25} Correlates with Appearance of AEP Enzyme Activity—We investigated further the relationship between removal of the N- and C-terminal propeptides and the appearance of enzyme activity *in vitro*. We generated various mutant forms of AEP, expressed them in 293T cells, and purified them from the culture supernatant. Following a shift to pH 4.0, we assessed autocatalytic processing and the appearance of enzyme activity. As previously reported (25) mutation of the active site cysteine residue Cys^{189} or of Asn^{323}, the target for removal of the C-terminal propeptide, blocked autocatalytic processing and the appearance of enzyme activity (Fig. 4, *a* and *b*). However, in the case of the Asn^{323} mutant, we consistently observed the appearance of enzyme activity following long incubations at pH 4.0 (Fig. 4*b*, *filled circles*). N-terminal sequencing of this mutant indicated that the appearance of enzyme activity correlated with cleavage at Asp^{25}. For example, after a 16-h incubation, 34% of the protein had the mature N terminus (GGKHW), and 36% of wild type enzyme activity had appeared. This suggests that cleavage at Asn^{323}, although profoundly rate-limiting, is not essential for enzyme activity. To test directly the need for cleavage at Asp^{25}, we performed a further experiment with the N323A mutant where the reversible inhibitor of AEP, Fmoc-AENK-amide, was included during the slow time course of activation and then diluted out, and enzyme activity was assessed at pH 5.8. As shown in Fig. 4*c*, the appearance of enzyme activity was abolished under these conditions (Fig. 4*c*), providing further evidence that cleavage at Asp^{25} is required. As expected, the inhibitor also profoundly slowed the activation of the wild type enzyme as well.

We next tested the effect of mutating Asp^{25}. Because after shorter times of autoactivation we also observed a small mole fraction of the N-terminal sequence DPEDG indicating cleavage after Asp^{21} (Fig. 2*c*), we also mutated this residue. In fact this mutation made little difference either to autocatalytic processing (Fig. 4*a*) or to the appearance of enzyme activity (Fig. 4*b*). In contrast mutation of Asp^{25} (with or without simultaneous mutation of Asp^{21}) led to the appearance of a slower migrating 47-kDa species upon shift to pH 4.0, confirming that Asp^{25} is recognized during autocatalytic cleavage of the N-terminal propeptide *in vitro* (Fig. 4*a*). When we examined the appearance of enzyme activity, the rate of autoactivation of the D25A and D21A,D25A mutants was significantly slower (Fig. 4*b*). Nonetheless, given the data already described correlating cleavage at Asp^{25} with appearance of enzyme activity, we were surprised that the Asp^{25} mutants activated as well as they did. One possibility is that the mutation not only prevents cleavage but also disrupts an important interaction of the N-terminal propeptide with the enzyme. To try to address this we tested the effect of adding back to activated enzyme the wild type 8-mer peptide or variants thereof. As shown in Fig. 4*d*, the wild type sequence VPIDDPED was able to inhibit AEP hydrolysis of the Z-AAN-NHMec substrate and indeed the pH-triggered autocatalytic cleavage of wild type AEP (Fig. 4*e*). In contrast, a randomized version of the same sequence was completely inactive. Moreover, a peptide that corresponded to the D21A,D25A mutant (VPIADPEA) also failed to inhibit AEP activity as did the Asp to Glu variant VPIEDPEE. These results show that the N-terminal propeptide can act as a specific inhibitor of the active enzyme, although fairly high concentrations are required. In addition, this experiment is consistent with the hypothesis that mutagenesis of Asp^{25} may not only block autocatalytic cleavage but also the ability of this sequence to interact effectively with the enzyme. This may explain why enzyme activity appeared to the extent it did with the Asp^{25} mutant.

Visualization of Active and Inactive AEP in Living Cells—We asked whether inactive and active forms of AEP might be visualized in living cells. Because the levels of AEP in most

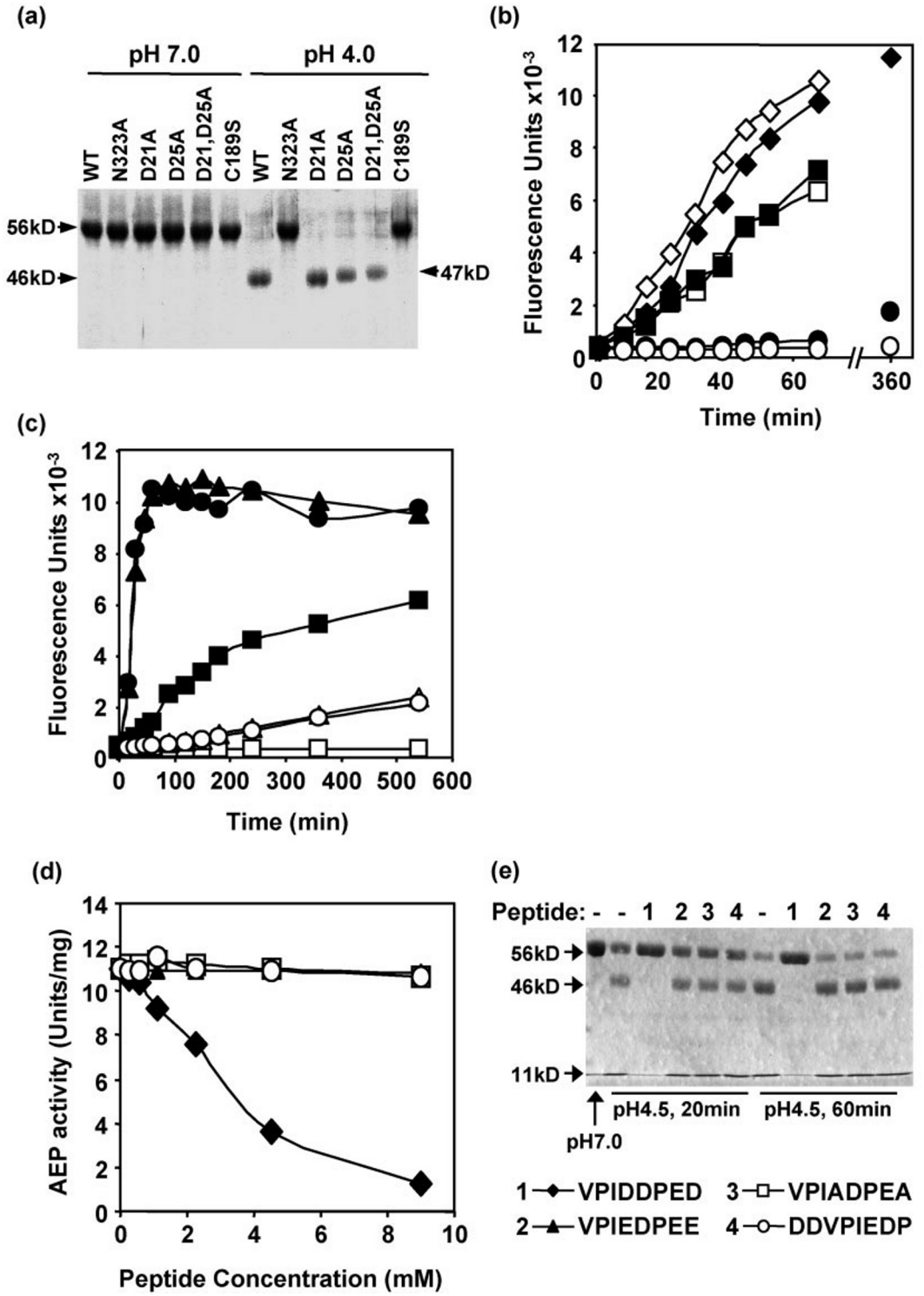

FIG. 4. **Removal of the N-terminal propeptide correlates with AEP activation.** *a*, purified wild type and various mutant AEP precursors (shown at pH 7.0) were incubated at pH 4.0 under conditions that lead to autoactivation of the wild type AEP precursor. The Coomassie Blue-stained gel demonstrates failure of the D25A and D21A,D25A mutants to generate the 46-kDa form. *b*, time course of appearance of AEP activity for wild type (♦) and D21A (◇), D21A,D25A (■), D25A (□), N323A (●), and C189S (○) mutant forms. *c*, wild type (*filled symbols*) or N323A proAEP was incubated at pH 4.0 at a concentration of 0.5 mg·ml^{-1} in the presence of the reversible inhibitor Fmoc-AENK-amide (■ and □) or a control peptide, Fmoc-AEQK-amide (▲ and △). The autoactivation reaction was stopped by diluting into pH 5.8 buffer and further diluted into assay buffer for measurement of AEP enzyme activity. The final concentration of inhibitor peptide in the assay buffer was 2.3 μM, *i.e.* less than 10% that of the Z-Ala-Ala-NHMec substrate, which was adjusted to 25 μM. As control for this residual inhibitor, the control peptide-treated samples were also adjusted to 2.3 μM AENK (● and ○). *d* and *e*, the N-terminal propeptide VPIDDPED and variant forms VPIEDPEE, VPIADPEA, and DDVPIEDP were included at the concentrations shown in a standard AEP assay at pH 5.8 (*d*) and added to an AEP autoactivation experiment (*e*). The extent of autoactivation was assessed on Coomassie Blue-stained gels.

cells are too low to permit visualization of transient maturation intermediates, we used a previously described melanoma cell line SD1 (12) that overexpresses AEP, although not to the extent seen in the CHO cell lines. Because of background problems with the N-terminus-specific rabbit serum, we purified a subfraction of the polyclonal sheep serum using the

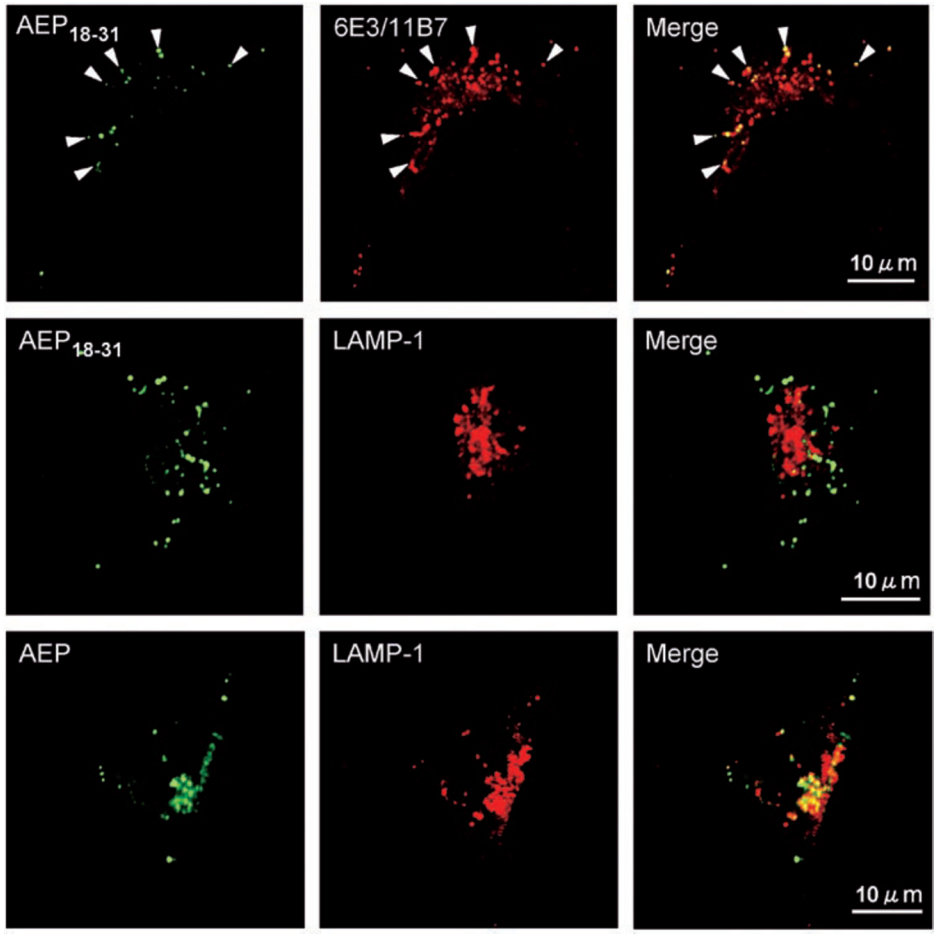

FIG. 5. **The precursor and active forms of AEP reside in distinct intracellular compartments.** The AEP overexpressing cell line MelJuSo-SD1 was stained as indicated with sheep anti-AEP or anti-AEP_{18-31} (*green*) and a mixture of the AEP-specific monoclonal antibodies 6E3 and 11B7 or anti-LAMP-1 (*red*) and analyzed by confocal microscopy. The *arrowheads* in the *top panels* identify a subset of compartments that contain inactive proenzyme. Magnification, ×100.

immobilized N-terminal peptide as adsorbent (see "Materials and Methods"). We were able to isolate antibodies that only reacted with the 56- and 47-kDa forms of AEP and that labeled a distinct set of compartments in living SD1 cells. All of these compartments were also labeled by a mixture of two monoclonal mouse anti-AEP antibodies, 11B7 and 6E3, reactive with all forms of AEP (Fig. 5 and data not shown). However, the latter antibodies also identified a second set of compartments that were not labeled by the N-terminal pro-peptide-specific antibodies. These vesicles occupied a more perinuclear position and, unlike most of the compartments labeled by the propeptide specific antibodies, were LAMP-1-positive and therefore presumably lysosomes (Fig. 5). Thus there is heterogeneity among the endosomal/lysosomal compartments harboring the AEP protease; some clearly contain significant levels of the precursor forms, whereas others, which are mostly LAMP-1 positive, appear to have fully converted the enzyme to the mature form by removal of the N-terminal propeptide.

Evidence That AEP Autoactivation Can Proceed in a Bimolecular Fashion—In the case of the papain-like C1 family of lysosomal cysteine proteases, the precise mechanism of autoactivation has been difficult to pin down with both unimolecular and bimolecular mechanisms being proposed (33–36). In a bimolecular reaction, the rate of appearance of enzyme activity should accelerate over time and be sensitive to the concentration of proenzyme. 56-kDa AEP, at various concentrations, was shifted to pH 4.5, and autoactivation was allowed to proceed for different times, after which the enzyme was diluted in pH 5.8 assay buffer, preventing further autoactivation. As shown in Fig. 6*a*, the rate of appearance of enzyme activity accelerated with time, consistent with a bimolecular mechanism. In addition, the rate of appearance of enzyme activity was markedly sensitive to pro-enzyme concentration. At 40 μg/ml almost 10% of the enzyme had become activated in 10 min, whereas at 1 μg/ml only about 0.5% had been activated (Fig. 6*b*).

A bimolecular mechanism should allow catalytically inactive enzyme to be processed in the presence of active enzyme. We tested this in living CHO cells by feeding exogenous ^{125}I-labeled wild type AEP or mutant C189S AEP. As shown in Fig. 6*c*, both forms of the enzyme were taken up, were processed to the mature 36-kDa size, and were precipitable with sheep serum but not with the rabbit serum raised against the N-terminal pro-peptide. Presumably, the C189S mutant is processed by endogenous active AEP in a bimolecular fashion. We performed the same experiment in the monocytic cell line THP-1, which has low levels of endogenous AEP.[3] These cells took up the AEP precursor very inefficiently but nonetheless revealed that although there was some processing of the mutant enzyme, a partially processed form precipitable with the rabbit antiserum also accumulated, *i.e.* retaining the N-terminal propeptide (Fig. 6*c*). Thus the rate of AEP processing *in vivo* is also dependent upon AEP activity. In the case of C189S, which has no intrinsic enzyme activity, there is sufficient endogenous AEP to catalyze efficient bimolecular processing in CHO cells but not in THP-1. Conversely, the wild type enzyme is equally efficiently processed in either cell type.

Taken together the data are consistent with a bimolecular mechanism of AEP activation both *in vitro* and *in vivo*. This does not, however, exclude the possibility that a unimolecular process can proceed at a slower rate and may precede a bimolecular phase.

[3] B. Manoury and S. P. Matthews, unpublished observation.

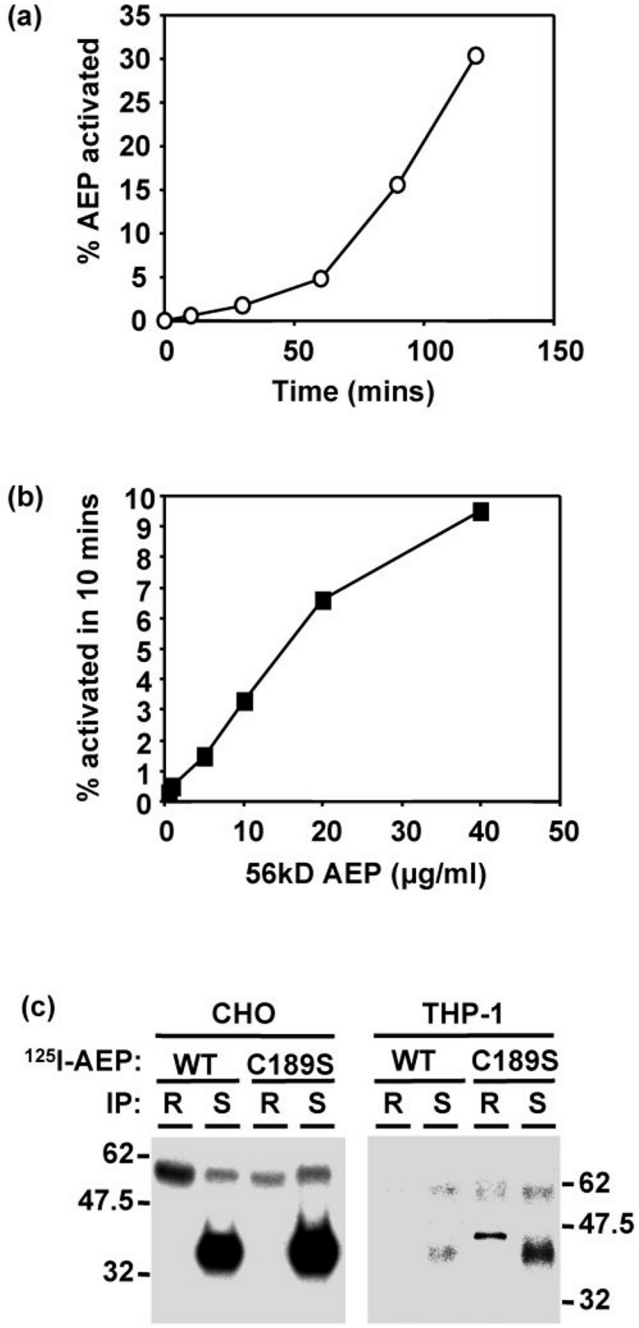

FIG. 6. **AEP autoactivation is a bimolecular reaction.** *a*, the AEP precursor (1 μg/ml) was shifted to pH 4.5 to trigger autoactivation. At each time point identical amounts of enzyme (5 ng) were transferred to pH 5.8 assay buffer, and an AEP activity assay was performed for 20 min. *b*, AEP precursor was shifted to pH 4.5 at the different concentrations shown, and autoactivation was allowed to proceed for 10 min. Equal amounts of enzyme were transferred to an AEP assay at pH 5.8 as in *a*. To compare the extent of activation at different concentrations of 56-kDa precursor, the activity obtained in 2 h at a concentration of 40 μg/ml was set to 100% because under these conditions AEP was fully activated. *c*, CHO cells and THP-1 cells were incubated for 6 h in the presence of 0.2 μg/ml ^{125}I-labeled 56-kDa wild type (*WT*) or C189S AEP. Captured AEP was sequentially immunoprecipitated by first rabbit (*R*) and then sheep (*S*) antisera and visualized by SDS-PAGE and autoradiography.

Activation of AEP Is Regulated during Dendritic Cell Maturation—Cells may need to regulate the proteolytic capacity of their endosome/lysosome system under different conditions. This could be controlled at the level of protease expression by expression of endogenous inhibitors such as cystatins (37) or by regulation of zymogen activation, which, as shown above, can progress in a stepwise fashion with different potential regulatory points. There is evidence that DC may use cystatins to modulate their cysteine protease activity and that this may contribute to regulation of class II MHC expression following LPS-driven maturation of immature DC (38). Using serial analysis of gene expression Hashimoto *et al.* (39) have observed that AEP/legumain expression is induced as monocytes differentiate into macrophages. We therefore asked whether AEP maturation was regulated during human DC development and maturation.

$CD14^+$ monocytes from human peripheral blood were cultured in granulocyte macrophage colony-stimulating factor plus interleukin-4. At intervals, the cells were removed for analysis of AEP induction and maturation state by Western blotting. After 6 days, half of the cells were exposed to LPS to drive maturation. For reasons that are not clear, the results of this analysis were somewhat variable from donor to donor in terms of levels of AEP induction. Nonetheless, as shown in Fig. 7 (*left panel*), in DC from some donors we could observe a clear induction of AEP expression during the culture period consistent with the serial analysis of gene expression of Ref. 39. Interestingly, following LPS challenge, there was a clear disappearance of the 56-kDa inactive form and a corresponding increase in the fully active 36-kDa form. This general pattern was replicated in a second experiment (Fig. 7, *right panel*) in which the effect of LPS was examined after 16 and 40 h. Once again, there was a clear conversion of inactive AEP to active enzyme. Thus in primary dendritic cell cultures the induction and activation of AEP can be regulated by appropriate physiological stimuli.

DISCUSSION

Mammalian AEP, also known as mammalian legumain, is a lysosomal cysteine protease unrelated to the papain-like lysosomal cathepsins. It has unusually precise specificity for cleavage after asparagine and selectivity even among asparagine containing sequences (1, 10, 41). It is involved in both immune and autoimmune antigen processing reactions (10–14) and also can perform activating cleavages in other substrates such as progelatinase A and prothymosin α (17, 18). All of the evidence to date indicates that AEP has evolved to introduce limited cleavages into folded protein substrates. The plant form of AEP, legumain, has also been shown to be responsible for pro-protein activation (42). How this enzyme is itself activated is therefore of some interest. In agreement with previous work, we find that activation is autocatalytic and triggered by acidic pH (21–25). Using highly purified human proenzyme, we show in addition that activation is bimolecular and requires the sequential removal of C- and N-terminal propeptides at different pH thresholds by cleavage after asparagine 323 and aspartic acid 25, respectively. Several considerations support the conclusion that the latter is the key activating cleavage. First, the inactive 47-kDa form was extended by 8 N-terminal residues relative to the active 46-kDa form. Second, incubation of the N323A AEP mutant at activating pH resulted in very slow appearance of enzyme activity that nonetheless correlated with cleavage at Asp^{25}. The reversible inhibitor AENK blocked both this cleavage and the appearance of enzyme activity. Third, the addition of the 8-mer N-terminal propeptide, VPIDDPED, to active enzyme inhibited the enzyme in a dose-dependent fashion. Randomization of this peptide or alteration of the key terminal Asp residue prevented inhibition. Finally, the N-terminal sequence we observe for the active 46-kDa form fits precisely with the known N terminus of the enzyme isolated from mammalian cells (1).

We believe that our results can reconcile the somewhat dis-

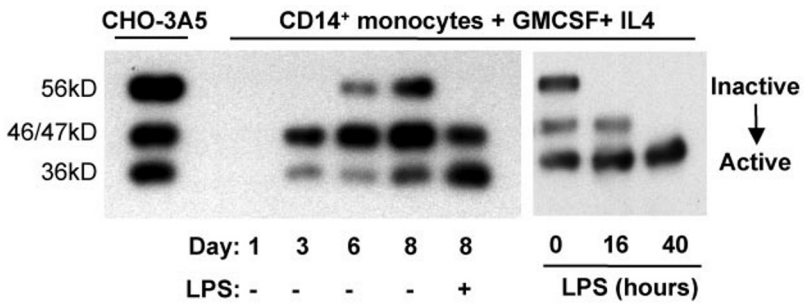

FIG. 7. **Induction and maturation of AEP in monocyte-derived dendritic cells.** Dendritic cells, differentiated from CD14+ blood monocytes, were analyzed for AEP content and size by Western blotting on days 1, 3, 6, and 8 as shown. Where indicated LPS was added on day 6 for 48 h (*left panel*) or times shown (*right panel*). CHO-3A5 cell lysate is run in the *leftmost lane* to provide standards for the three major AEP forms.

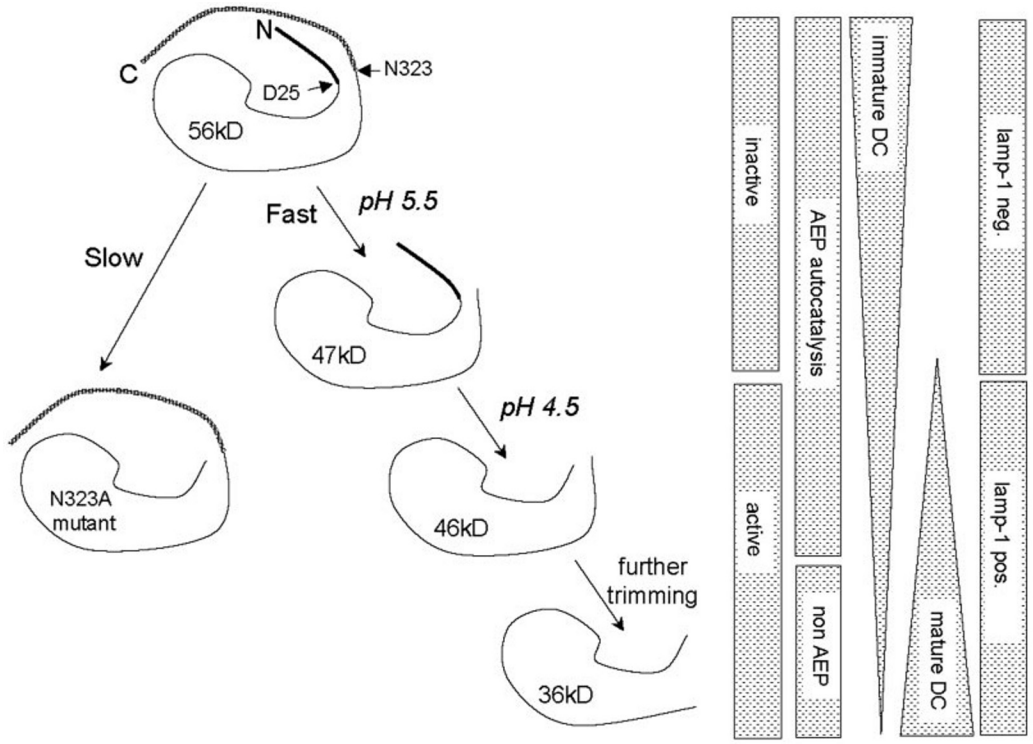

FIG. 8. **Suggested scheme for cellular processing of AEP.** The inactive 56-kDa proenzyme, resident in prelysosomal compartments, is progressively converted to active 46-kDa AEP by sequential autocatalytic cleavage at Asn^{323} followed by Asp^{25}. Subsequent C-terminal trimming by other lysosomal proteases yields the final mature 36-kDa form but does not result in any further increase in enzyme activity. Autoactivation is highly pH-dependent and may in part be controlled by endosomal acidification or progress through the endosome/lysosome system, because the 56/47-kDa species are not present in LAMP-1^+ vesicles. This represents a possible mechanism for the control of AEP activation during maturation of monocyte-derived dendritic cells.

crepant earlier reports on activation of mammalian AEP/legumain. These studies reported autocatalytic cleavages after either aspartic acid or asparagine (24, 25). We find that both are required. Halfon *et al.* (24) observed several autocatalytic cleavages at aspartic residues in an AEP-Ig fusion protein, but it was not clear which were activating. In contrast Chen *et al.* (25) demonstrated the same autocatalytic cleavage at Asn^{323} that we report here, and they also detected an additional increase in mobility below pH 5.0 concomitant with enzyme activation. However, they attributed this to further processing at the C terminus and concluded that removal of residues at the N terminus was not necessary for activity. However, a second C-terminal processing event to account for enzyme activation seems more difficult to envisage because there is no Asn (or Asp) residue upstream of Asn^{323} that could be autocatalytically cleaved to account for the size reduction observed from 47 to 46 kDa. The present data bear comparison with those of Kuroyanagi *et al.* (21), who reported a similar stepwise removal of C-terminal followed by N-terminal propeptides during autoactivation of the *Arabidopsis* AEP, γVPE. Interestingly, however, this plant enzyme differs from mammalian AEP in that both cleavages are made after Asn, and the acquisition of enzyme activity correlates solely with cleavage at the C terminus.

Our data support a scheme for AEP autoactivation summarized in Fig. 8. The key autoactivating cleavage occurs not after asparagine but after aspartic acid. Moreover, this cleavage only occurs at lower pH values. One possibility is that lower pH is required to protonate the aspartate side chain, thus making it resemble an asparagine side chain. Indeed, a synthetic peptide corresponding to residues 18–31 of pro-AEP (VPIDDPEDGGKHWV) was hydrolyzed more efficiently by activated AEP at pH 4.0 than at pH 5.8 (data not shown). Other residues in this very acidic sequence may also need to be protonated. Both the major Asp^{25} and the minor Asp^{21} processing sites we observed are preceded in the P3 position by proline. Interestingly, other studies have noted some preference for proline in the P3 posi-

tion before canonical Asn cleavage sites (41, 43). Detection of cleavage at Asp^{21} suggests that two sequential cleavages at Pro-Xaa-Asp motifs can occur, each removing 4 amino acids. Because the 8-mer peptide is inhibitory, cleavage in two steps might serve to inactivate it. However, mutagenesis of Asp^{21} did not affect the appearance of enzyme activity, so cleavage at this site is not obligatory. Below pH 3.0, the activating cleavage at Asp^{25} was no longer observed. Possibly the titration of other residues around the active site now precludes autocatalysis at Asp^{25}. We have also noted that AEP can cleave some protein substrates at Asp residues.[2]

Lysosomal cysteine proteases of the papain family are generally autoactivated following removal of a single long (50–100 residues) N-terminal propeptide (44–47). In this context AEP is unusual in requiring the removal of two propeptides, one C-terminal and one N-terminal. Nor are there close similarities with the activation pathways of the other cysteine proteases in clan CD. These include the caspases, separase, and gingipain. Caspases differ in their mode of activation with executioner caspases (*e.g.* caspases 3 and 7) being activated by single proteolytic cleavages performed by upstream "apical" caspases (*e.g.* caspases 8 and 9) (48). Recent data suggest that the latter are not primarily activated by cleavage but rather by dimerization, with cleavage conferring other properties such as stability and sensitivity to inhibitors (49). In the case of separase, cleavages occur but may not be essential for activity (50). The activation of Arg-gingipain has also recently been analyzed *in vitro*. Like AEP, activation requires autocatalytic removal of both N- and C-terminal propeptides (51). However, the order of removal is reversed, with removal of a 229-residue N-terminal peptide preceding removal of 72 residues at the C terminus. Unlike AEP, the zymogen form of Arg-gingipain showed significant catalytic activity (51).

Similar to Arg-gingipain, the rate of AEP autoactivation was sensitive to the concentration of the precursor, suggesting that activation proceeds most efficiently as a bimolecular (*i.e.* intermolecular rather than intramolecular) process. In the case of the lysosomal cathepsins whose autoactivation has been studied, both unimolecular and bimolecular mechanisms have been proposed (33–36). However, for those procathepsins whose structures are known (cathepsins B, L, and K) (44–47), a bimolecular mechanism is favored because the active site, which is fully formed in the proenzyme, is distant from the pro/mature junction site(s) that are cleaved during autoactivation. In addition the propeptide passes through the active site cleft in the opposite orientation to a normal substrate peptide. Nonetheless, evidence has been recently presented for an activated intermediate for cathepsin B and S where the propeptide was cleaved not at the pro/mature junction but rather upstream at sites that are known (cathepsin B) or predicted (cathepsin S) to be in close proximity to the catalytic center (36). This cleavage, despite the reversed orientation, was postulated to be a unimolecular event. Thus the relative contributions of unimolecular and bimolecular events in cathepsin activation are not fully resolved. In the case of AEP, evidence for a bimolecular process was found both *in vitro* and *in vivo*. It remains possible, however, that there is also a unimolecular pathway. Structural analysis of the different intermediate forms should help resolve some of these outstanding questions.

It is intriguing to speculate that cells might exploit the pH-staged activation of enzymes like AEP to regulate proteolysis. For example, it is known that in immature DC antigen can be endocytosed and stored for several days in an unprocessed form (52, 53). Upon maturation of the cells, for example with LPS, the antigen (hen egg lysozyme in the best studied case) is processed and the peptides are loaded onto class II MHC. In addition to differential expression of endogenous protease inhibitors such as cystatin C (38) and variations in class II MHC trafficking patterns (54, 55), regulation of protease activation might also contribute to altered antigen processing and presentation as dendritic cells mature. We show here that AEP biosynthesis is induced as monocytes differentiate into dendritic cells, confirming earlier results from serial analysis of gene expression (39). However, we found that immature DC can harbor significant amounts of inactive AEP. Upon LPS-driven maturation, AEP activation is completed. Trombetta *et al.* (56) have recently reported a similar phenomenon in murine DC and have also shown that such enhanced proenzyme processing and enhanced antigen processing capacity is due to enhanced acidification of the endosome/lysosome system. Thus by setting pH thresholds for activation of protease zymogens, cells may fine tune the proteolytic capacity of the endocytic pathway to meet particular biological requirements. The pathway of AEP activation described here offers a clear example of this.

Acknowledgments—We thank Thomas Friedberg, Simon Powis, Vas Ponnambalam, and David Williams for advice and reagents, Nick Morrice and David Campbell for protein sequencing, Sarah Blackwood for monoclonal antibody screening, and Cathy Moss for helpful comments on the manuscript.

REFERENCES

1. Chen, J. M., Dando, P. M., Rawlings, N. D., Brown, M. A., Young, N. E., Stevens, R. A., Hewitt, E., Watts, C., and Barrett, A. J. (1997) *J. Biol. Chem.* **272,** 8090–8098
2. Turk, B., Turk, D., and Turk, V. (2000) *Biochim. Biophys. Acta* **1477,** 98–111
3. Shutov, A. D., Do, N. L., and Vaintraub, I. A. (1982) *Biokhimiia* **47,** 814–821
4. Hara-Nishimura, I., Takeuchi, Y., and Nishimura, M. (1993) *Plant Cell* **5,** 1651–1659
5. Kembhavi, A. A., Buttle, D. J., Knight, C. G., and Barrett, A. J. (1993) *Arch. Biochem. Biophys.* **303,** 208–213
6. Klinkert, M. Q., Felleisen, R., Link, G., Ruppel, A., and Beck, E. (1989) *Mol. Biochem. Parasitol.* **33,** 113–122
7. Dalton, J. P., Hola Jamriska, L., and Brindley, P. J. (1995) *Parasitology* **111,** 575–580
8. Uhlmann, F., Wernic, D., Poupart, M. A., Koonin, E. V., and Nasmyth, K. (2000) *Cell* **103,** 375–386
9. Chen, J. M., Rawlings, N. D., Stevens, R. A. E., and Barrett, A. J. (1998) *FEBS Lett.* **441,** 461–365
10. Manoury, B., Hewitt, E. W., Morrice, N., Dando, P. M., Barrett, A. J., and Watts, C. (1998) *Nature* **396,** 695–699
11. Antoniou, A. N., Blackwood, S. L., Mazzeo, D., and Watts, C. (2000) *Immunity* **12,** 391–398
12. Manoury, B., Mazzeo, D., Fugger, L., Viner, N., Ponsford, M., Streeter, H., Mazza, G., Wraith, D. C., and Watts, C. (2002) *Nat. Immunol.* **3,** 169–174
13. Anderton, S. M., Viner, N. J., Matharu, P., Lowrey, P. A., and Wraith, D. C. (2002) *Nat. Immunol.* **3,** 110–112
14. Beck, H., Schwarz, G., Schroter, C. J., Deeg, M., Baier, D., Stevanovic, S., Weber, E., Driessen, C., and Kalbacher, H. (2001) *Eur. J. Immunol.* **31,** 3726–3736
15. Lennon-Dumenil, A. M., Bakker, A. H., Wolf-Bryant, P., Ploegh, H. L., and Lagaudriere-Gesbert, C. (2002) *Curr. Opin. Immunol.* **14,** 15–21
16. Manoury, B., Mazzeo, D., Li, D. N., Billson, J., Loak, K., Benaroch, P., and Watts, C (2003) *Immunity* **18,** 489–498
17. Chen, J. M., Fortunato, M., Stevens, R. A., and Barrett, A. J. (2001) *Biol. Chem.* **382,** 777–783
18. Sarandeses, C. S., Covelo, G., Diaz-Jullien, C., and Freire, M. (2003) *J. Biol. Chem.* **278,** 13286–13293
19. Choi, S. J., Reddy, S. V., Devlin, R. D., Menaa, C., Chung, H., Boyce, B. F., and Roodman, G. D. (1999) *J. Biol. Chem.* **274,** 27747–27753
20. Shirahama-Noda, K., Yamamoto, A., Sugihara, K., Hashimoto, N., Asano, M., Nishimura, M., and Hara-Nishimura, I. (May 29, 2003) *J. Biol. Chem.* 10.1074/jbc.M302742200
21. Kuroyanagi, M., Nishimura, M., and Hara-Nishimura, I. (2002) *Plant Cell Physiol.* **43,** 143–151
22. Hiraiwa, N., Nishimura, M., and Hara-Nishimura, I. (1999) *FEBS Lett.* **447,** 213–216
23. Caffrey, C. R., Mathieu, M. A., Gaffney, A. M., Salter, J. P., Sajid, M., Lucas, K. D., Franklin, C., Bogyo, M., and McKerrow, J. H. (2000) *FEBS Lett.* **466,** 244–248
24. Halfon, S., Patel, S., Vega, F., Zurawski, S., and Zurawski, G. (1998) *FEBS Lett.* **438,** 114–118
25. Chen, J. M., Fortunato, M., and Barrett, A. J. (2000) *Biochem. J.* **352,** 327–334
26. Lanzavecchia, A. (1985) *Nature* **314,** 537–539
27. Ding, S., Yao, D., Burchell, B., Wolf, C. R., and Friedberg, T. (1997) *Arch. Biochem. Biophys.* **348,** 403–410
28. Johansen, H. T., Knight, C. G., and Barrett, A. J. (1999) *Anal. Biochem.* **273,** 278–283
29. Sallusto, F., and Lanzavecchia, A. (1994) *J. Exp. Med.* **179,** 1109–1118
30. Schimke, R. T., Kaufman, R. J., Alt, F. W., and Kellems, R. F. (1978) *Science*

202, 1051–1055.21
31. Kaufman, R. J., Bertino, J. R., and Schimke, R. T. (1978) *J. Biol. Chem.* **253,** 5852–5860
32. Rome, L. H., Weissmann, B., and Neufeld, E. F. (1979) *Proc. Natl. Acad. Sci. U. S. A.* **76,** 2331–2334
33. Mach, L., Mort, J. S., and Glossl, J. (1994) *J. Biol. Chem.* **269,** 13030–13035
34. Menard, R., Carmona, E., Takebe, S., Dufour, E., Plouffe, C., Mason, P., and Mort, J. S. (1998) *J. Biol. Chem.* **273,** 4478–4484
35. Rozman, J., Stojan, J., Kuhelj, R., Turk, V., and Turk, B. (1999) *FEBS Lett.* **459,** 358–362
36. Quraishi, O., and Storer, A. C. (2001) *J. Biol. Chem.* **276,** 8118–8124
37. Alvarez-Fernandez, M., Barrett, A. J., Gerhartz, B., Dando, P. M., Ni, J., and Abrahamson, M. (1999) *J. Biol. Chem.* **272,** 19195–19203
38. Pierre, P., and Mellman, I. (1998) *Cell* **93,** 1135–1145
39. Hashimoto, S., Suzuki, T., Dong, H. Y., Yamazaki, N., and Matsushima, K. (1999) *Blood* **94,** 837–844
40. Hashimoto, S., Suzuki, T., Dong, H. Y., Nagai, S., Yamazaki, N., and Matsushima, K. (1999) *Blood* **94,** 845–852
41. Dando, P. M., Fortunato, M., Smith, L., Knight, C. G., McKendrick, J. E., and Barrett, A. J. (1999) *Biochem. J.* **339,** 743–749
42. Yamada, K., Shimada, T., Kondo, M., Nishimura, M., and Hara-Nishimura, I. (1999) *J. Biol. Chem.* **274,** 2563–2570
43. Mathieu, M. A., Bogyo, M., Caffrey, C. R., Choe, Y., Lee, J., Chapman, H., Sajid, M., Craik, C. S., and McKerrow, J. H. (2002) *Mol. Biochem. Parasitol.* **121,** 99–105
44. Coulombe, R., Grochulski, P., Sivaraman, J., Menard, R., Mort, J. S., and Cygler, M. (1996) *EMBO* **15,** 5492–5503
45. Cygler, M., Sivaraman, J., Grochulski, P., Coulombe, R., Storer, A. C., and Mort, J. S. (1996) *Structure* **4,** 405–416
46. Podobnik, M., Kuhelj, R., Turk, V., and Turk, D. (1997) *J. Mol. Biol.* **271,** 774–788
47. LaLonde, J. M., Zhao, B., Janson, C. A., D'Alessio, K. J., McQueney, M. S., Orsini, M. J., Debouck, C. M., and Smith, W. W. (1999) *Biochemistry* **38,** 862–869
48. Earnshaw, W. C., Martins, L. M., and Kaufmann, S. H. (1999) *Annu. Rev. Biochem.* **68,** 383–424
49. Boatright, K. M., Renatus, M., Scott, F. L., Sperandio, S., Shin, H., Pedersen, I. M., Ricci, J. E., Edris, W. A., Sutherlin, D. P., Green, D. R., and Salvesen, G. S. (2003) *Mol. Cell* **11,** 529–541
50. Waizenegger, I., Gimenez-Abian, J. F., Wernic, D., and Peters, J. M. (2002) *Curr. Biol.* **12,** 1368–1378
51. Mikolajczyk, J., Boatright, K. M., Stennicke, H. R., Nazif, T., Potempa, J., Bogyo, M., and Salvesen, G. S. (2003) *J. Biol. Chem.* **278,** 10458–10464
52. Inaba, K., Turley, S., Iyoda, T., Yamaide, F., Shimoyama, S., Reis e Sousa, C., Germain, R. N., Mellman, I., and Steinman, R. M. (2000) *J. Exp. Med.* **191,** 927–936
53. Turley, S. J., Inaba, K., Garrett, W. S., Ebersold, M., Unternaehrer, J., Steinman, R. M., and Mellman, I. (2000) *Science* **288,** 522–527
54. Cella, M., Engering, A., Pinet, V., Pieters, J., and Lanzavecchia, A. (1997) *Nature* **388,** 782–787
55. Villadangos, J. A., Cardoso, M., Steptoe, R. J., van Berkel, D., Pooley, J., Carbone, F. R., and Shortman, K. (2001) *Immunity* **14,** 739–749
56. Trombetta, E. S., Ebersold, M., Garrett, W., Pypaert, M., and Mellman, I. (2003) *Science* **299,** 1400–1403